Structural and Spectroscopic Study of the Dihydrogen Bond in an Imine Triosmium Complex

S. Aime,*,[†] E. Diana,[†] R. Gobetto,[†] M. Milanesio,[‡] E. Valls,[§] and D. Viterbo[‡]

Dipartimento Chimica I.F.M., Università di Torino, Via P. Giuria 7, 10125 Torino, Italy, Dipartimento di Scienze e Tecnologie Avanzate, Università del Piemonte Orientale, Corso T. Borsalino 54, 15100 Alessandria, Italy, and Unitat de Quimica Inorganica, Universitat Autonoma de Barcelona, 08193 Bellaterra, Spain

The presence of an intramolecular XH···HM interaction between the imine proton donor and the terminal hydride in $H(\mu\text{-}H)Os_3(CO)_{10}(HN=CPh_2)$ has been investigated by X-ray analysis, NMR and IR spectroscopy and theoretical calculations. The localization of the hydrogen atoms in the crystal structure yielded a H···H distance of 1.79(6) Å for this "unconventional" H···H interaction; theoretical calculations suggested an H···H distance of 1.89 Å in the solid state. A NMR determination of the interproton distance, obtained from the isolation of the selective H,H dipolar contribution to the hydride relaxation time, afforded a value of 2.00 ± 0.05 Å. The difference between NMR and solid state determinations may be explained on the basis of the occurrence, in solution, of a large amplitude oscillatory motion of the imine ligand along the N−Os coordination axis. Further evidence of the presence of the favorable N−H···H−M intramolecular hydrogen bond interaction has been obtained from the red shift of the $\nu(N-H)$ stretching in $H(\mu\text{-}H)Os_3(CO)_{10}(HN=CPh_2)$ with respect to that of the related $Os_3(CO)_{11}(HN=CPh_2)$ compound. DFT(B3LYP) calculations gave results in agreement with the experimental findings and allowed further insight into the nature of the N−H···H−M dihydrogen bond, pinpointing the electrostatic nature of this interaction and the role of the high polarizability of the Os−H bond.

Introduction

The recent observation of a new type of dihydrogen bond (DHB) between hydrides (M−H) and classical hydrogen donor groups, such as N−H or O−H, represents an important step toward the understanding of the role of weak interactions in determining the stereochemistry and reactivity of organometallic systems.[1−5]

The M−H···H−X (X = O, N) linkage may be either intra- or intermolecular, and the H···H distance has been reported to be as small as 1.7 Å.[6]

Theoretical investigations of the DHB in main group elements[7,8] and in monometallic systems[9] provided a first rationalization scheme to classify these interactions as "unconventional" hydrogen bonds. In particular, Orlova and Scheiner have demonstrated that such H···H interaction is favored in the case of poor and moderate proton donors H−X and a strong π acceptor trans ligand.[9] It is easy to foresee that a better understanding of the role of these kinds of interactions may contribute to a better design of reagents and catalysts in organometallic chemistry.

We have suggested that the Os−H···H−N interaction is responsible for driving the stereochemistry in a series of adducts containing primary and secondary amines coordinated to a triosmium cluster.[10,11] Moreover it has been found that the addition of aldehydes or ketones to the ammonia-containing derivative leads to the formation of terminally coordinated imine ligands which are stabilized through the same type of interactions.[12]

Herein we present an in-depth experimental (using IR, NMR, and X-ray data) and theoretical characterization of the Os−H···H−N DHB in the trimetallic cluster $H(\mu\text{-}H)Os_3(CO)_{10}(HN=CPh_2)$ (**1** in Chart 1), reporting the first crystal structure, in which Os−H acts as H-bond acceptor, with an H···H distance below 2.0 Å; this interaction is the shortest H···H distance, among the Os−H···H−X contacts, found in the Cambridge Structural Database (CSD).[13] Our findings allow us to get a more detailed picture of the structural and

† Università di Torino.
‡ Università del Piemonte Orientale.
§ Universitat Autonoma de Barcelona.
(1) (a) Lee, J. C.; Peris, E.; Rheingold, A. L.; Crabtree R. H. *J. Am. Chem. Soc.* **1994**, *116*, 11014−11019. (b) Lee, J. C.; Rheingold, A. L.; Muler, B.; Pregosin, P. S.; Crabtree, R. H. *J. Chem. Soc., Chem. Commun.* **1994**, 1021−1022. (c) Park, S.; Ramachandran, R.; Lough, A. J.; Morris, R. H. *J. Chem. Soc., Chem. Commun.* **1994**, 2201−2202.
(2) Crabtree, R. H.; Siegbahn, P. E. M.; Eisenstein, O.; Rheingold A. L.; Koetzle, T. F. *Acc. Chem. Res.* **1996**, *29*, 348−354, and references therein.
(3) Belkova, N. V.; Shubina, E. S.; Ionidis, A. V.; Epstein, L. M.; Jacobsen, H.; Messmer, A.; Berke, H. *Inorg. Chem.* **1997**, *36*, 1522−1525.
(4) Peris, E.; Lee, J. C.; Rambo, J. R.; Eisenstein, O.; Crabtree, R. H. *J. Am. Chem. Soc.* **1995**, *117*, 3485−3491.
(5) Custelcean, R.; Jackson, J. E. *Chem. Rev.* **2001**, *101*, 1963−1980.
(6) Braga, D.; Grepioni, F.; Tedesco, E.; Calhorda, M. J.; Lopes, P. E. M. *New J. Chem.* **1999**, 219−226, and references therein.
(7) Kulkarni, S. A.; Srivastava, A. K. *J. Phys. Chem. A* **1999**, *103*, 2836−2842.
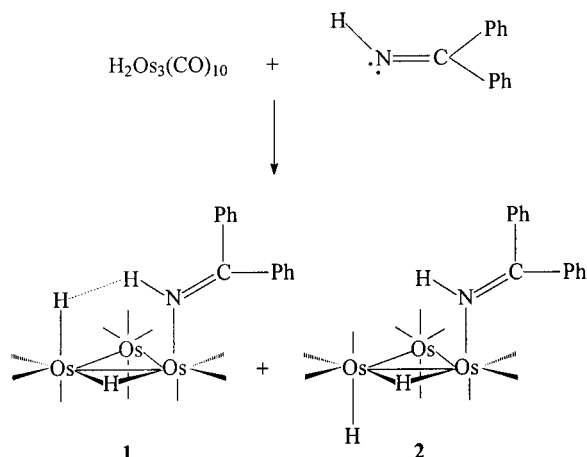(8) Grabowsky, S. J. *J. Phys. Chem. A* **2000**, *104*, 5551−5557.
(9) Orlova, G.; Scheiner, S. *J. Phys. Chem. A* **1998**, *102*, 260−269.

(10) Aime, S.; Gobetto, R.; Valls, E. *Organometallics* **1997**, *16*, 5140−5141.
(11) Aime, S.; Ferriz, M.; Gobetto, R.; Valls, E. *Organometallics* **2000**, *19*, 707−710.
(12) Aime, S.; Ferriz, M.; Gobetto R.; Valls, E. *Organometallics* **1999**, *18*, 2030−2032.

Chart 1

electronic determinants of the formation of a DHB on the surface of a triosmium cluster.

Experimental Section

Syntheses and NMR Data. All solvents were dried and stored over molecular sieves. $(\mu\text{-H})_2Os_3(CO)_{10}$[14] and $Os_3(CO)_{11}$-$(NCCH_3)$[15] were prepared according to published procedures.

[13]CO metal carbonyls were prepared by using as starting material ^{13}C-enriched (ca. 20%) $Os_3(CO)_{12}$ obtained by direct exchange of [13]CO with $Os_3(CO)_{12}$ in *n*-octane at 110 °C for 3 days in sealed vials.[16] [13]CO (99% enriched) was purchased from Isotec (Miamisburg, OH). ^{1}H and ^{13}C NMR spectra were recorded on a JEOL EX-400 spectrometer operating at 399.65 and 100.24 MHz, respectively. Nonselective inversion recovery pulse sequences were used to obtain [1]H T_1 values.[17] The samples for T_1 measurements were degassed using freeze−pump−thaw techniques. The temperature was calibrated with a standard methanol ^{1}H thermometer sample.[15] Errors in the reported T_1 values were estimated to be in the range ±2%. The accurate determination of the interproton distances has been obtained by fitting the experimental T_1 vs $1/T$ and by applying the reported equations (vide infra).

Synthesis of $H(\mu\text{-H})Os_3(CO)_{10}(HN=CPh_2)$ (Chart 1). In a typical reaction 5 mg of $(\mu\text{-H})_2Os_3(CO)_{10}$ (5.9×10^{-6} mol) in 0.5 mL of CD_2Cl_2 was transferred into a 5 mm NMR tube, and an excess of $Ph_2C=NH$ was added. The solution color readily turned from purple to yellow. ^{1}H NMR (CD_2Cl_2, 400 MHz, 218 K): δ 9.87 (N*H*), 7.67−7.28 (aromatic), −9.90 (d, $^3J = 2.8$ Hz, H2), −15.85 (d, $^3J = 2.8$ Hz, H3). IR (CH_2Cl_2 solution, carbonyl region): 2100(m), 2074(w,sh), 2062(s), 2049(s), 2021(ms), 2004-(ms), 1983 (m,sh), 1964 (m,sh).

Synthesis of $Os_3(CO)_{11}(HN=CPh_2)$. $Os_3(CO)_{11}(NCCH_3)$ (10 mg) dissolved in 1 mL of dichloromethane was allowed to react with an equimolar amount of benzophenone imine (HN= CPh_2). Complete conversion to $Os_3(CO)_{11}(HN=CPh_2)$ occurs in a few minutes, and the compound was characterized by ^{1}H and ^{13}C data. ^{1}H NMR (CD_2Cl_2, 400 MHz, 193 K): δ 9.22 (N*H*) 7.30−7.65 (aromatic). ^{13}C NMR for the carbonyl resonances (CD_2Cl_2, 400 MHz, 193 K): δ 188.9 (2) ($^2J_{C,C} = 34.6$ Hz), 185.2 (2) ($^2J_{C,C} = 34.6$ Hz), 182.2 (1), 177.9 (2), 175.2 (2), 174.3 (2).

Table 1. Summary of Crystal Data and Structure Refinement Parameters for 1

formula	$C_{23}H_{13}NO_{10}Os_3$
fw	1033.94
cryst syst	triclinic
space group	$P\bar{1}$
a	8.013(1) Å
b	11.324(1) Å
c	15.004(2) Å
α	84.067(2)°
β	80.878(2)°
γ	77.391(2)°
V	1308.6(2) Å³
Z	2
$F(000)$	932
density (calc)	2.624 g cm⁻³
temp	293(2) K
diffractometer	SMART-CCD
radiation (graph monochr.)	0.71073 Å
abs coeff	14.583 mm⁻¹
cryst size	$0.14 \times 0.10 \times 0.05$ mm
color	orange
shape	triangular plate
scan method	ω
frame width	0.30°
time per frame	30 s
no. frames	2400
detector−sample distance	2.95 cm
θ range	1.38−30.53
index ranges	$-11 \leq h \leq 11$, $-16 \leq k \leq 16$, $-21 \leq l \leq 21$
no. reflns collected	23 300
no. ind reflns	7948 [R(int) = 0.0417]
abs corr (SADABS) av redundancy	2.93
max.−min. transmn	0.156−0.039
refinement method	full-matrix least-squares on $\|F_o\|^2$
no. obsd reflns	5947 [$I>2\sigma(I)$]
no. data/restraints/params	7948/1/346
goodness-of-fit on $\|F_o\|^2$	0.880
R indices [$I>2\sigma(I)$]	R1 = 0.0237, wR2 = 0.0471
R indices (all data)	R1 = 0.0356, wR2 = 0.0481
largest diff peak and hole	1.307, −1.108 e Å⁻³
weight (calcd)	$w = 1/[\sigma^2(\|F_o\|^2) + (P)^2]$, $P = (\|F_o\|^2 + 2\|F_c\|^2)/3$

IR ($CHCl_3$ solution, carbonyl region): 2096(w), 2077(w,sh), 2066(s), 2044(s), 2019(s,br), 2001(s,br).

IR Analysis. IR spectra were recorded as CH_2Cl_2 or $CHCl_3$ solution for the carbonyl stretching region and as KBr pellets for the other spectral regions on a Bruker FTIR spectrophotometer model Equinox 55.

Crystal Structure Analysis. Crystals of the syn isomer (**1** in Chart 1) of $H(\mu\text{-H})Os_3(CO)_{10}(HN=CPh_2)$ suitable for X-ray analysis were obtained by evaporation of a hexane/chloroform solution. Crystallographic data and details of data collection and refinement are given in Table 1. Single-crystal diffraction data were collected at RT on a Bruker SMART CCD area detector diffractometer, using graphite-monochromatized Mo Kα (λ = 0.71073 Å) radiation.[18]

Absorption correction was performed using SADABS.[19] The structure was solved by direct methods (SIR97)[20] and refined by full-matrix least-squares (SHELX97).[21] Anisotropic thermal parameters were assigned to all the non-hydrogen atoms.

(13) Allen, F. H.; Kennard, O. *Chem. Des. Autom. News* **1993**, *8* (1), 1 & 31.

(14) Kaesz, H. D. *Inorganic Synthesis*; Angelici, R. J., Ed.; John Wiley & Sons: New York, 1990; Vol. 28, p 238.

(15) Nicholls, J. N.; Vargas, M. D. *Inorganic Synthesis*; Angelici, R. J., Ed.; John Wiley & Sons: New York, 1990; Vol. 28, p 232.

(16) Aime, S.; Milone, L.; Osella, D.; Sappa, E. *Inorg. Chim. Acta* **1978**, *29*, 2211−2218.

(17) Martin, M. L.; Delpuech, J. J.; Martin, G. J. In *Practical NMR Spectroscopy*; Heyden: London, 1980.

(18) Low-temperature data were collected on a larger crystal using our diffractometer with a scintillation counter, but the data were even more severely affected by absorption. We then decided to use a much smaller crystal on a CCD diffractometer where low temperature was not available, because absorption is a much greater problem than thermal motion.

(19) Sheldrick, G. M. *SADABS*; University of Göttingen: Germany, 1996.

(20) Altomare, A.; Burla, M. C.; Camalli, M.; Cascarano, G. L.; Giacovazzo, C.; Guagliardi, A.; Moliterni, A. G.; Polidori, G.; Spagna, R. *J. Appl. Crystallogr.* **1999**, *32*, 115−1134 (web site: http://www.ba.cnr.it/IRMEC/SirWare_main.htm).

Hydrogens bonded to the metals were located in a difference Fourier synthesis, using the structure refined with anisotropic displacement factors and reflections with $2\theta < 40°$. Aromatic and iminic hydrogens were set in calculated positions, after checking that they were present in the difference Fourier synthesis. Final atomic coordinates and temperature factors, together with all the other crystallographic information have been deposited.[22]

Theoretical Calculations. Ab initio Hartree−Fock[23] (HF) SCF-MO calculations[24] on the *syn*-(**1**) and *anti*-(**2**) isomers (Chart 1) and on some simple adducts (vide infra) were performed using the Gaussian98[25] program. The initial geometry of **1** was obtained from the X-ray analysis, and that of **2** was achieved by graphical manipulation of **1**. Geometrical optimizations were carried out at Hartree−Fock level, using Stuttgart RSC ECP pseudo-potentials and related basis set[26] for the Os atoms, the 6-31+G(d,p)[23] basis set for the H···H contact region, and the 3-21G[23] basis set for the remaining part of the molecule. Single-point energy calculations were carried out at the DFT level by adopting the hybrid B3-LYP functional, including the exchange part proposed by Becke[27] and the correlation functional proposed by Lee et al.[28] Stuttgart RSC ECP[26] for the Os atoms, 6-311++G(2d,2p)[23] for the H···H contact region, and 6-31G(d)[23] for the remaining part of the molecule were employed.

The graphic analysis was performed using the MOLDRAW[29] and the XP[30] programs, while the retrieval of the related structures was from the CSD.[13]

Rigid energy scans around selected bonds were carried out using the simple potential functions implemented in MOLDRAW.[29]

Results

Routes to imino metal complexes are usually based on the modification of previously coordinated ligands such as nitriles, oximes, and amines.[31] In polynuclear derivatives these reactions lead invariantly to systems in which the organic ligand occupies a bridging position.[32] The direct use of imines as ligands is hindered by the difficulty of avoiding their polymerization reac-

tion also under mild experimental conditions. Only benzophenone imine is stable enough to allow its use in reactions with metal carbonyls.[33]

The reaction between the coordinatively unsaturated $(\mu\text{-H})_2Os_3(CO)_{10}$ cluster and $HN{=}CPh_2$ proceeds readily at room temperature with a dramatic change in color from violet to pale yellow. This reaction is conveniently carried out in the NMR tube and turns out to be sensitive to the type of solvent.

In CD_2Cl_2 a single product corresponding to $H(\mu\text{-H})\text{-}Os_3(CO)_{10}(HN{=}CPh_2)$ (**1**) is obtained, as clearly demonstrated by the ^{13}C NMR spectrum of a [13]CO-enriched sample at 218 K which shows 10 carbonyl resonances of equal intensity at δ 185.5 ($^2J_{C-C}$ = 34.9 Hz), 184.3 ($^2J_{C-C}$ = 34.9 Hz), 180.3 ($^2J_{C-H}$ = 20.8 Hz), 175.9, 175.2, 174.9, 173.3, 173.1, 172.7 ($^2J_{C-H}$ = 12.8 Hz), and 168.7 ($^2J_{C-H}$ = 10.8 Hz), respectively. A partial assignment of the carbonyl resonances is straightforward on the basis of the $^2J_{C-C}$ and $^2J_{C-H}$ couplings. For instance, the two lowest field resonances showing the carbon−carbon coupling pattern correspond to the axial carbonyls in the rear $Os(CO)_4$ unit. The carbonyl trans to the terminal hydride falls at 180.3 ppm, whereas the resonances at 172.7 and 168.7 ppm correspond to carbonyls trans to the bridging hydride. When the temperature is increased, a small broadening and shift of most of the resonances (more evident for the resonances at δ 180.3 and 172.7) followed by their sharpening is observed. In analogy with what was previously observed for other $H(\mu\text{-H})Os_3(CO)L$ complexes,[34] this behavior can be explained with the exchange of the syn- and anti-isomers of $H(\mu\text{-H})Os_3(CO)_{10}(HN{=}CPh_2)$ (**1** and **2** in Chart 1). In fact a dynamic process involving the two hydrides and the two carbonyls which show the more pronounced broadening is responsible for the mutual exchange of the syn-isomer with the minor (nondetectable in CD_2Cl_2) anti-isomer.

As previously[11] observed in related derivatives, when $H(\mu\text{-H})Os_3(CO)_{10}(HN{=}CPh_2)$ is dissolved in polar solvents (i.e., acetone) the two isomers are formed in equimolar amounts. In CD_2Cl_2 solution, the intramolecular Os−H···H−N interaction drives the stereochemistry of the adduct, whereas the competition of acetone to act as proton acceptor leads to an equimolecular distribution of the two isomers. In acetone the activation barrier for the exchange between the syn- and anti-isomer corresponds to ca. 13.9 kcal/mol, as calculated from the band shape analysis as a function of temperature. In carrying out this determination, the monitor-

(21) Sheldrick G. M. *SHELXL-97*; University of Göttingen: Germany, 1997 (web site: http://shelx.uni-ac.gwdg.de/SHELX/).

(22) Supporting Information (coordinates of H atoms, anisotropic thermal parameters, bond distances and angles) has been deposited by the Cambridge Crystallographic Data Centre, with deposition number CCDC163107.

(23) Hehre, W. J.; Radom, L.; Schleyer, P.v. R.; Pople, J. A. *Ab Initio Molecular Orbital Theory*, 1st ed.; John Wiley & Sons: New York, 1986; Chapter 4.

(24) Various platforms, among which the IBM SP3 and O3K supercomputers of CINECA (www.cineca.it), were employed, because of the large size of the model system.

(25) Frisch, M. J.; Trucks, G. W.; Schlegel, H. B.; Scuseria, G. E.; Robb, M. A.; Cheeseman, J. R.; Zakrzewski, V. G.; Montgomery, J. A., Jr.; Stratmann, R. E.; Burant, J. C.; Dapprich, S.; Millam, J. M.; Daniels, A. D.; Kudin, K. N.; Strain, M. C.; Farkas, O.; Tomasi, J.; Barone, V.; Cossi, M.; Cammi, R.; Mennucci, B.; Pomelli, C.; Adamo, C.; Clifford, S.; Ochterski, J.; Petersson, G. A.; Ayala, P. Y.; Cui, Q.; Morokuma, K.; Malick, D. K.; Rabuck, A. D.; Raghavachari, K.; Foresman, J. B.; Cioslowski, J.; Ortiz, J. V.; Stefanov, B. B.; Liu, G.; Liashenko, A.; Piskorz, P.; Komaromi, I.; Gomperts, R.; Martin, R. L.; Fox, D. J.; Keith, T.; Al-Laham, M. A.; Peng, C. Y.; Nanayakkara, A.; Gonzalez, C.; Challacombe, M.; Gill, P. M. W.; Johnson, B. G.; Chen, W.; Wong, M. W.; Andres, J. L.; Head-Gordon, M.; Replogle, E. S.; Pople, J. A. *Gaussian 98*, revision A.7; Gaussian, Inc.: Pittsburgh, PA, 1998.

(26) Andrae, D.; Haeussermann, U.; Dolg, M.; Stoll, H.; Preuss, H. *Theor. Chim. Acta* **1990**, 77, 123. STUTTGART ECPs are available at the address: http://www.theochem.uni-stuttgart.de/.

(27) Becke, A. D. *J. Chem. Phys.* **1993**, 98, 5648−5652.

(28) Lee, C.; Yang, W.; Parr, R. G. *Phys. Rev. B* **1988**, 37, 785−789.

(29) Ugliengo, P.; Viterbo, D.; Chiari, G. *Z. Kristallogr.* **1993**, 207, 9−23 (web site: http://www.ch.unito.it/ifm/fisica/moldraw/moldraw.html).

(30) Sheldrick G. M. *SHELXTL/IRIS*; Bruker Analytical X-Ray Systems, Inc.: Madison, WI, 1990.

(31) (a) Mehrota, R. C. In *Comprehensive Organometallic Chemistry*; Wilkinson, G., Gillard, R. D., McCleverty, J. A., Eds.; Pergamon: Oxford, U.K., 1987; Vol. 2, pp 279−281. (b) Prenzler, D. P.; Hockless, D. C. R.; Heath, G. A. *Inorg. Chem.* **1997**, 36, 5845−5849. (c) Francisco, L. W.; White, P. S.; Templeton, J. L. *Organometallics* **1996**, 15, 5127−5136. (d) Balley, P. J.; Grant, K. J.; Pace, S.; Parsons, S.; Stewart, L. J. *J. Chem. Soc., Dalton Trans.* **1997**, 4263−4270. (e) Esteruelas, M. A.; Lahoz, F. J.; López, A. M.; Oñate, E.; Oro, L. A. *Organometallics* **1995**, 14, 2496−2500.

(32) (a) Farmery, K.; Kilner, M.; Midcalf, C. *J. Chem. Soc. A* **1970**, 2279−2285. (b) Kilner, M. Midcalf, C. *J. Chem. Soc., Dalton Trans.* **1974**, 1620−1626. (c) Andrews, M. A.; Van Burkirk; G. Knobler, C. B.; Kaesz, H. D. *J. Am. Chem. Soc.* **1979**, 101, 7245−7254. (d) Adams, R. D.; Katahira, D. A.; Yang, L. W. *J. Organomet. Chem.* **1981**, 219, 241−249. (e) Kohler, J. U.; Lewis, J.; Raithby, P. R.; Rennie, M. A. *Organometallics* **1997**, 16, 3851−3854.

(33) (a) Andreu, P. L.; Cabeza, J.A.; del Rio, I.; Riera, V.; Bois, C. *Organometallics* **1996**, 15, 3004−3010. (b) Cabeza, J. A.; del Rio, I.; Grepioni, F.; Riera, V. *Organometallics* **2000**, 19, 4643−4646.

(34) Keister J. B.; Shapley, J. R. *Inorg. Chem.* **1982**, 21, 3304−3310.
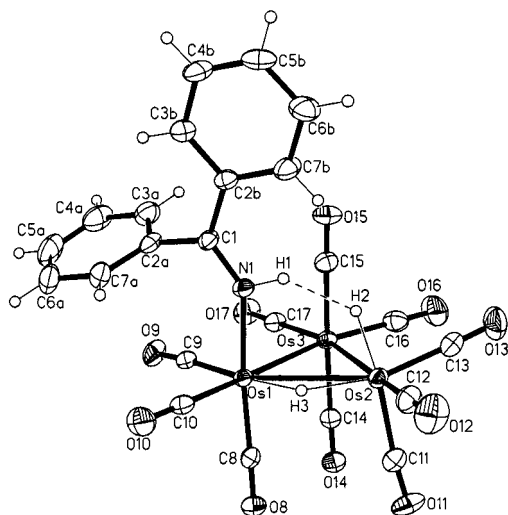
Figure 1. Drawing of the molecular structure of compound **1**, showing the adopted labeling scheme, with displacement ellipsoids drawn at the 30% probability level.

ing of the coalescence process of the imine protons of the two isomers at δ 10.59 and 10.83, respectively (rather than the corresponding hydride resonances), proves to be particularly useful since the smaller inner separation allows the observation of the fully collapsed spectrum.

The H–H distance in the Os–H···H–N linkage has been first evaluated in solution by extracting the dipolar contribution to the relaxation rate of the terminal hydride arising from the imine proton. This procedure consists of comparing the relaxation rates of the protio- and deuterio-isotopomers.[31,32] The H(μ-H)Os$_3$(CO)$_{10}$-(^{2}HN=CPh$_2$) isotopomer was prepared by addition of deuterated benzophenone imine to a CD$_2$Cl$_2$ solution of (μ-H)$_2$Os$_3$(CO)$_{10}$. The interatomic H···H distance can then be obtained from $1/(T_{1,D})^{H-H}$ according to the following equations:

$$\frac{1}{T_{1,D}}^{H-H} = \left[\frac{1}{T_1(protio)} - \frac{1}{T_1(deuterio)} \right] \times 1.0625 \quad (1)$$

$$\frac{1}{T_{1,D}}^{H-H} = \frac{3\gamma_H^4 \hbar^2 \tau_c}{10 r_{H-H}^6} \left[\frac{1}{1 + \tau_c^2 \omega_0^2} + \frac{4}{1 + 4\tau_c^2 \omega_0^2} \right] \quad (2)$$

Particularly reliable values of the molecular correlation time (τ_c) are obtained when the T_1 of the hydride resonance displays its minimum value. At the operating frequency of 400 MHz (ω_0), T_1 minimum (0.47 s) is obtained at ca. 208 K. At this temperature $\tau_c = 0.62/\omega_0$ (in rad s^{-1}); thus $\tau_c = 2.45 \times 10^{-10}$ rad s^{-1}. When this value is introduced in eq 2, an $r_{H,H}$ distance of 2.00 ± 0.05 Å is obtained.

X-ray Crystal Structure of 1. The molecular structure of **1** is shown in Figure 1, and selected bond lengths and angles are presented in Table 2.

The syn disposition of the hydride H2 and of the imine is confirmed. The observed Os2–H2 distance of 1.56(5) Å is one the smallest among those reported from X-ray data on related derivatives in the Cambridge Database. More reliable Os–H bond distances, ranging from 1.57[35] to 1.67[36] Å, can be retrieved from neutron data. The presence of an axial hydrogen instead of a bulkier ligand

Table 2. Selected Bond Lengths (Å) and Angles (deg) for Complex 1

Distances	
Os(1)–N(1)	2.150(4)
Os(1)–Os(3)	2.9077(4)
Os(1)–Os(2)	2.9958(3)
Os(1)–H(3)	1.67(4)
Os(2)–Os(3)	2.8804(3)
Os(2)–H(2)	1.56(5)
Os(2)–H(3)	1.78(4)
N(1)–H(1)	0.958(19)

Angles	
N(1)–Os(1)–Os(3)	91.47(10)
N(1)–Os(1)–Os(2)	85.29(10)
Os(3)–Os(1)–Os(2)	58.38(1)
N(1)–Os(1)–H(3)	82.0(16)
Os(3)–Os(1)–H(3)	89.3(16)
Os(2)–Os(1)–H(3)	31.0(15)
Os(3)–Os(2)–Os(1)	59.28(1)
Os(3)–Os(2)–H(2)	76.6(18)
Os(1)–Os(2)–H(2)	73.3(19)
Os(3)–Os(2)–H(3)	88.2(14)
Os(1)–Os(2)–H(3)	28.9(14)
H(2)–Os(2)–H(3)	77(2)
Os(2)–Os(3)–Os(1)	62.34(1)
Os(1)–N(1)–H(1)	111(3)

causes some distortions in the Os$_3$(CO)$_{10}$ moiety, with respect to the pseudo-C_3-symmetry of Os$_3$(CO)$_{12}$. The angles between the Os1–Os2–Os3 plane and the carbonyl groups C12 and C13 linked to Os2 are Os1–Os2–Os3/Os2–C12–C13 = 14.3°, Os1–Os2–Os3/Os2–C12 = 5.4°, and Os1–Os2–Os3/Os2–C13 = 12.6°, respectively. The corresponding angles at Os1 and Os3 are much closer to zero (0.2–1.2°). Of the two phenyl groups of the benzophenonimine ligand, one is almost parallel to the Os1–Os2–Os3 plane ("equatorial"), while the other is almost perpendicular ("axial").

The most relevant structural information is indeed the short H···H distance in the Os–H- - -H–N linkage [1.79(6) Å]. It could be argued that a dihydrogen distance measured from X-ray data may be rather inaccurate, but in our complex the H1 position is dictated by the stereochemistry of the imine group and the electron-rich H2 is clearly detectable from the difference Fourier map. Some theoretical calculations (see Theoretical Calculations section below) were performed to confirm such a short H- - -H distance. The angular distortions of the ligands on Os2 contribute to the shortening of the distance between the interacting hydrogen atoms.
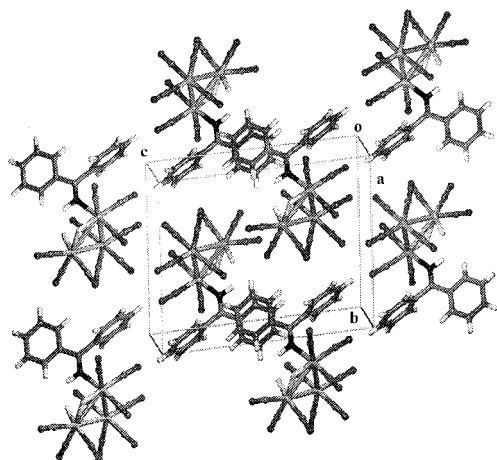
Also the overall crystal packing (Figure 2) shows interesting features as it is driven by stacking interactions between "axial" phenyl groups (phenyl–phenyl distance 3.7 Å) and by six C–H···OC intermolecular contacts[37] (average and minimun H···O distance of 2.83 and 2.66 Å, respectively). Such a distance suggests that these contacts can be ascribed to vdW interactions, since the sum of vdW radii of H and C is 2.87 Å.

Estimate of the DHB Bonding Energy by IR Analysis. The stretching vibration of the N–H group

(35) Maltby, P. A.; Sclaf, M.; Steinbeck; M.; Lough, A. J.; Morris, R. H.; Klooster, W. T.; Koetzle; T. F.; Sristava, R. C. *J. Am. Chem. Soc.* **1996**, *118*, 5396–5407.

(36) (a) Hart, D. W.; Bau, R.; Koetzle, T. F. *J. Am. Chem. Soc.* **1977**, *99*, 7557–7564. (b) Johnson, T. J.; Albinati, A.; Koetzle, T. F.; Ricci, J.; Eisenstein, O.; Huffman, J. C.; Caulton, K. G. *Inorg. Chem.* **1994**, *33*, 4966–4976.

(37) Braga, D.; Grepioni, F.; Desiraju, G. T. *Chem. Rev.* **1998**, *98*, 1375. See in particular section V-D and references therein.

Figure 2. Crystal packing of H(μ-H)Os$_3$(CO)$_{10}$(HN=CPh$_2$) (**1**).

Figure 3. Comparison of the IR spectra, in the NH stretching region, of H(μ-H)Os$_3$(CO)$_{10}$(HN=CPh$_2$) (**1**) and of Os$_3$(CO)$_{11}$(HN=CPh$_2$).

Table 3. Geometrical Features (distances in Å and Angles in deg) of the H1···H2 Interaction in 1^a

	solid state		solution	
	1 X-ray structure	H-OPT model^b	NMR data	gas-phase model^c
H1···H2	1.79(6)	1.89	2.00(5)	1.93
N···H2	2.48(5)	2.68		2.69
Os2−H2	1.56(5)	1.67		1.67
N−H1···H2	127(4)	137		130
Os2−H2···H1	134(4)	119		113
Os1−Os2−H2	73(2)	84		85

^{a} The structural results from X-ray and NMR experimental data are compared with those from theoretical calculations. ^{b} H-OPT: only H1, H2, and H3 positions optimized. ^{c} Gas-phase: full geometry optimization, except Os−Os distances.

of the coordinated imine ligand may be used as an indicator of the strength of the DHB present in H(μ-H)Os$_3$(CO)$_{10}$(HN=CPh$_2$). Jogansen[38] proposed, for linear hydrogen bonds in organic molecules, the following empirical relation to obtain the value of the bonding enthalpy:

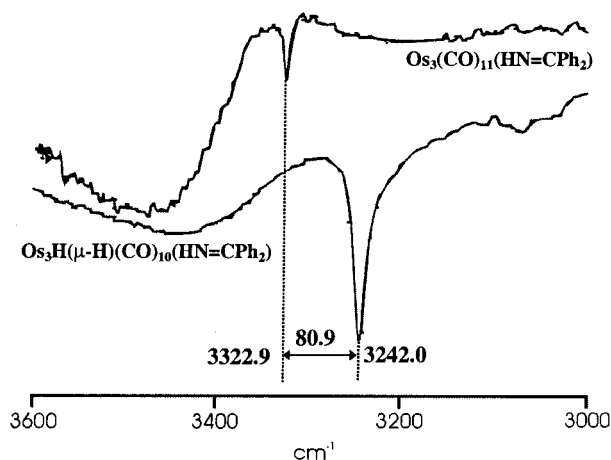$$-\Delta H = 18\Delta\nu_{NH}/(\Delta\nu_{NH} + 720) \text{ kcal/mol}$$

where $\Delta\nu_{NH}$ is the shift in stretching frequency due to the hydrogen bond. It was demonstrated that this relation may be used also for transition metal hydrides.[39]

To apply this procedure, it is necessary to know ν_{NH} of a reference compound with no DHB. To this purpose, Os$_3$(CO)$_{11}$(HN=CPh$_2$) (**3**) has been prepared (see Experimental Section) from the reaction of the "lightly stabilized" Os$_3$(CO)$_{11}$(NCCH$_3$) with benzophenone imine. Its structure may be envisaged as derived from Os$_3$(CO)$_{12}$ upon replacement of an axial carbonyl by the imine ligand. The synthesis and the spectroscopic data for this compound are reported in the Experimental Section.

On comparing the IR spectra of **1** and **3** in the 3000−3400 cm^{-1} region, it is evident that ν(NH) in **1** is shifted to lower wavenumbers (red shift), and it is increased in intensity in the presence of the DHB (Figure 3); this is the typical behavior of a "normal" hydrogen bond.

Introducing the observed $\Delta\nu_{NH}$ value of 80.9 cm^{-1} into eq 3, ΔH is evaluated to correspond to ca. 2.25 kcal/mol. In principle this approach is valid only for intermolecular interactions when the angle between the NH and the MH is close to 180°. In the case of H(μ-H)Os$_3$-(CO)$_{10}$(HN=CPh$_2$) this interaction occurs in a five-membered ring, and then it is likely that ring strain will affect ΔH. Nevertheless the obtained value is reasonable and in keeping with theoretical calculations (see Discussion).

Theoretical Calculations. The positions of the hydrogen atoms involved in the DHB and that of the bridging hydrogen (located with some uncertainty by the X-ray analysis) were checked by performing ab initio

MO calculations on the isolated molecule of isomers **1** and **2**. At first, only the positions of H1, H2, and H3 in **1** were optimized (H-OPT model in Table 3), while the rest of the structure was fixed at the X-ray geometry. Then all geometric parameters of isomers **1** and **2**, except for the Os−Os bond lengths, were optimized (gas-phase model in Table 3). The "H-OPT" approach can be considered as a good model for the study of the DHB in the solid state, while the gas-phase model can be considered as a suitable approximation of the molecules of **1** and **2** in a relatively nonpolar solvent such as CD$_2$Cl$_2$.

Calculations with the H-OPT model gave a H1···H2 distance of 1.89 Å, which is within 2σ with respect to the X-ray distance. Nevertheless, this calculated distance is larger than the X-ray one and seems more reasonable for a hydrogen bond presenting a $\Delta\nu_{NH}$ value of 80.9 cm^{-1}. Therefore, from now on, the calculated H1···H2 H-OPT distance of 1.89 Å will be considered as the most reasonable estimate of this H···H contact in the solid state.

Calculations with the H-OPT model gave an Os2−H2 distance of 1.67 Å (close to that from neutron diffraction.[35,36]), which is larger (but within 2σ) with respect to the X-ray distance. This lengthening alone cannot explain the different H1···H2 distance in the X-ray data and in the H-OPT model. In fact, this difference is mainly due to the different values ($\Delta > 5\sigma$ in Table 3) of the Os1−Os2−H2 angle in the X-ray structure and in the H-OPT model. As a result of this

(38) Iogansen, A. V. *Hydrogen Bond*; Nauka: Moskow, 1981; p 112.
(39) Shubina, E. S.; Belkova, N. V.; Krylov, A. N.; Vorontsov, E. V.; Epstein, L. M.; Gusev, D. G.; Niederman, M.; Berke, H. *J. Am. Chem. Soc.* **1996**, *118*, 1105−1112.
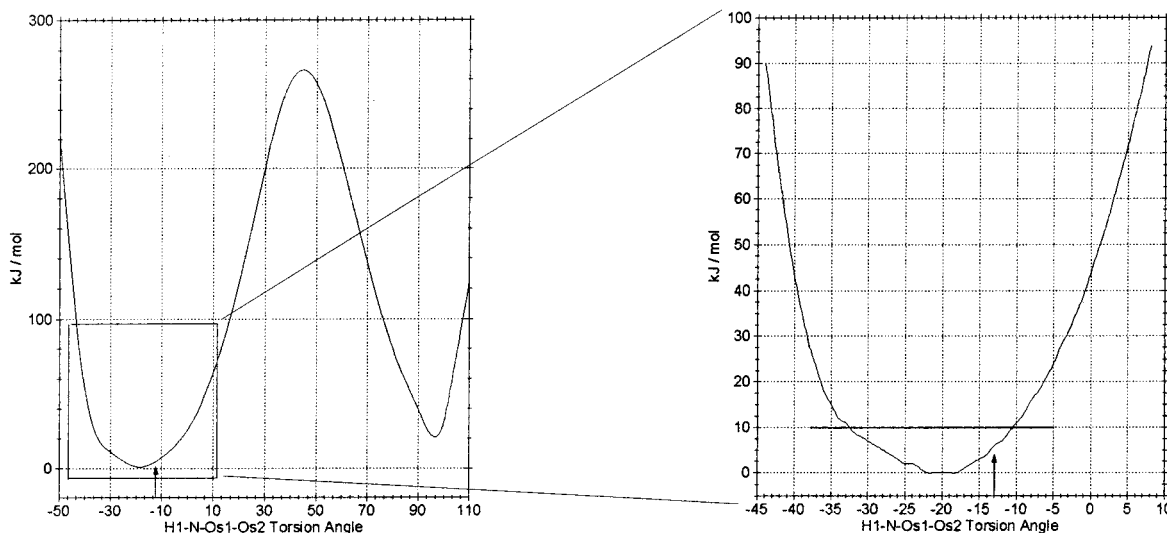
Figure 4. Energy barrier for the rotation of the imine group around the Os1−N bond in the angular range −50° to 110°.

angular difference, the Os2−H2 bond is more bent toward the imine group in the X-ray structure than in the H-OPT model. A significant angular distortion of the easily polarizable Os−H bond (see later) is not surprising.

The geometry optimization of **1** and **2** was performed with constraints only on the Os−Os distances (gas-phase in Table 3) and permitted us to further investigate the geometrical differences observed for **1** in solution (NMR data) and in the solid state (X-ray data) and to estimate the strength of the DHB. The structure of **1**, after geometry optimization of the X-ray structure, presents bond distances and angles, involving the DHB, closer to the standard values reported in the literature. In particular the Os2−H2 distance of 1.67 Å is within the range suggested by neutron data.[35,36] Nevertheless the substituents at Os2 remain tilted with respect to the Os1−Os2−Os3 plane.

Single-point calculations at the B3-LYP[27,28] level on the gas-phase geometry of **1** and **2** suggested that the DHB energy is weak (2.6 kcal/mol); they also permitted the estimation the Mullikan charges on H1 (+0.21) and H2 (−0.59), which suggest that an electrostatic component is important in this DHB.

Discussion

H···H Distance in the Dihydrogen Interaction.
In the solid state the H···H distance (1.89 Å, as estimated from the H-OPT model) is less than the sum of the vdW radii and proves that the N−H···H−Os contact is a genuine intramolecular interaction. A search in the CSD[13] showed that this value is among the shortest ones reported for this type of DHB in transition metal hydrides and the shortest one involving Os−H. In fact, many examples of compounds with an Os−H can be found in the CSD,[40] but no Os−H···H−X interactions in which the H···H distance is shorter than 2.25 Å were found. It is worth noting that the even weaker Os−H···H−C contacts are far more common[41] in the CSD, probably because CH-containing ligands are more commonly found in organometallic chemistry with respect to NH- or OH-containing ligands.

Relaxation time (T_1) NMR data in CD_2Cl_2 solution indicate a longer DHB with respect to the solid state.

The difference (0.1 Å) between the H···H distances in the Os−H···H−N linkage measured in the solid state [1.89 Å] and in solution [2.00 Å] cannot be only due to the occurrence of crystal packing effects or to an error in the determination of the H1 and H2 positions, as pointed out before. Also theoretical calculations with geometrical optimization (GP model) suggest a smaller H···H distance (1.93 Å), with respect to the NMR data. On the other hand the difference cannot be associated with inaccuracies of the NMR procedure, as the reliability of interatomic distances obtained by using dipolar relaxation data in a number of structural determinations has been proved by a number of studies.[42] To account for the occurrence of such a difference, we should consider that the H···H distance obtained from the NMR measurements represents an average value between exchanging structures; indeed a "static" structure could not be achieved even at the lowest attained temperature (208 K). One may therefore envisage an important role of the large amplitude motion of the imine ligand (without a complete rotation) which causes the H···H distance to span a rather large range of values. Indeed an energy scan around the Os1−N bond (Figure 4), carried out using MOLDRAW,[29] shows that there is a rather wide low-energy angular range. Within this range the H1···H2 distance varies between 1.79 and 1.99 Å.

Likely the conclusion that the NMR distance reflects a dynamic state of the DHB interaction has to be extended to all Os−H···H−N distances previously reported for related H(μ-H)Os$_3$(CO)$_{10}$(amine)[10] and H(μ-H)Os$_3$(CO)$_{10}$(imine)[11,12] systems.

Strength of the Dihydrogen Interaction. The strength of this intramolecular DHB is about 2.5 kcal/mol according to IR data and theoretical calculations, a value typical of very weak hydrogen bonds. The

(40) Braga, D.; Grepioni, F.; Tedesco, E.; Biradha, K.; Desiraju, G. R. *Organometallics* **1996**, *15*, 2692−2699.
(41) Seven structures (CSD[13] codes: BAKWIT, BOKCAF, CIDWER11, DACWUZ, DCTPHO, DEQBOQ, HELWOK) present OsH···HC contacts shorter than 2.0 Å, while no OsH···HX (X = O, N) with H···H shorter than 2.25 Å can be found in the CSD.
(42) (a) Kasaka, K. A.; Imoto, T.; Hatano, H. *Chem. Phys. Lett.* **1973**, *21*, 398−400. (b) Aime, S.; Botta, M.; Gobetto, R.; Osella, D. *Inorg. Chem.* **1987**, *26*, 2551−2552. (c) Aime, S.; Cisero, M.; Gobetto, R.; Osella, D.; Arce, A. J. *Inorg. Chem.* **1991**, *30*, 1614−1617.
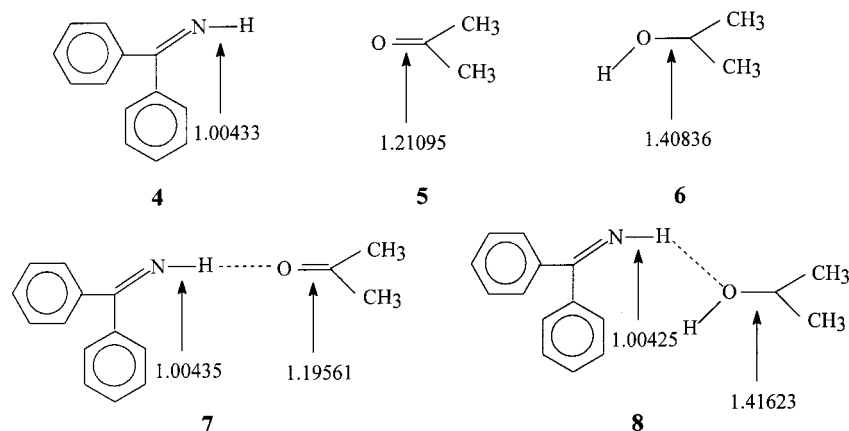
Figure 5. Relevant calculated bond lengths (in Å) for some "normally" H-bonded adducts (**7**, **8**) and for the related free molecules (**4**, **5**, **6**).

calculated values of the interaction energy and of the H⋯H distance for **1** are in keeping with the trend of the energy versus distance plot obtained from high-level MO calculations on a series of main group DHB complexes.[8] Only a limited number of examples of M−H⋯H−X (M: any transition metal, X: O or N) interactions showing H⋯H distances shorter than the sum of the vdW radii can be found in the CSD,[13] and this fact may support the weak nature of these inter- and intramolecular X−H⋯H−M interactions.

Nevertheless, these weak interactions are capable of affecting the relative yield of **1** (with DHB) and **2** (with no DHB) in solvents of different polarity, as reported above and extensively described in references 11 and 12 for related compounds.

Nature of the Dihydrogen Interaction. Electrostatic interactions, similar to those observed in "normal" X−H⋯X (X = O, N) hydrogen bonds (NHB), are expected to play an important role in an interaction between the positively charged iminic proton (H1) and a negatively charged hydride (H2). The charge distribution analysis in **1** obtained from B3-LYP calculations indicates Mullikan charges of opposite sign on H2 (−0.59) and on H1 (+0.21), confirming a relevant electrostatic contribution to the DHB. These calculated charges, although possibly affected by some error, support the view that in **1** H1 is a typical electron-depleted hydrogen apt to act as hydrogen bond donor, while H2 is an electron-rich hydrogen, apt to accept an H-bond. A charge rearrangement seems to be induced by DHB, as suggested by the smaller negative charge on H2 found in **2** (−0.34).

Experimental IR data confirm a red shift of ν(N−H) in **1** with respect to $Os_3(CO)_{11}(HN=CPh_2)$, and this fact suggests, within the applicability of the Jogansen formula,[38] that DHBs involving transition metal hydrides behave as "normal" hydrogen bonds. On the contrary, DHB differs from normal H bonds because of a larger contribution of the polarization component, as suggested by different theoretical works,[7] in which the Kitaura−Morokuma[43] energy decomposition technique was employed. The large polarizability of the Os2−H2 bond was experimentally confirmed by the significant red shift of the M−H stretching in the IR spectra, when

DHB is formed, reported by Shubina et al.[39] Indeed the calculated (gas-phase model, see Theoretical Calculations section for details) Os2−H2 distance is longer in **1** with respect to **2** (see Table 3).

To get more insight into the comparison between DHB and conventional hydrogen bonds, calculations at the HF/6-31G(d,p) level, with full geometry optimization, were undertaken on adducts **7** and **8** formed between benzophenoneimine (**4**) and acetone (**5**) or 2-propanol (**6**). In Figure 5 the relevant distances for the donor and acceptor moieties are reported as well as the corresponding ones obtained for the free molecules. No significant change is observed for the N−H bond length in the free or H-bonded benzophenoneimine; an analogous invariance of the N−H distance was found on passing from **2** to **1**. Conversely significant changes in the carbon−oxygen bond lengths have been detected in the acceptor molecule. In the case of acetone, the formation of the adduct **7** leads to a shortening of the C=O bond as the hydrogen-bonding interaction removes charge from π^*-orbitals. When the acceptor group is the OH group of 2-propanol, the expected elongation of the C−O bond in **8** occurs. This lengthening of +8 mÅ is very similar to that calculated for Os2−H on going from **2** to **1** (+6 mÅ). We can then see that the medium strength hydrogen bond in **8** has the same lengthening effect on the acceptor moiety of the weak DHB in **1**. It can therefore be inferred that the contribution of the polarizability of the metal hydrogen bond plays an important role[9] in the case of the interaction involving this group. It is worth recalling that the polarization of the M−H bond may be reversed, as it can act as H bond-acceptor (this work) or -donor,[40] depending upon the surrounding environment.

Insights into the Reactivity of 1. When a CD_2Cl_2 solution of **1** is allowed to react with $DN=CPh_2$ at room temperature for few minutes, there is the disappearance of both hydride resonances. The full deuteration of the terminal and bridging sites is further confirmed by the observation of the hydride resonances in the ^2D NMR spectrum at 213 K. This observation implies the reversible addition/dissociation of the imine ligand, coupled to the distribution of deuterium at both hydride positions. One may envisage a multistep process to account for the observed behavior. As depicted in Chart 2, the intramolecular DHB may evolve to the reversible for-

(43) Kitaura, K.; Morokuma, K. *Int. J. Quantum Chem.* **1976**, *10*, 325−340.

Chart 2
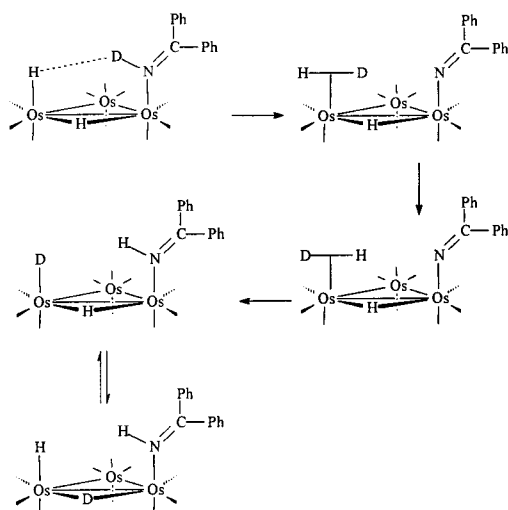
mation of a "nonclassical" hydride intermediate in which the rotation of the H−D molecule along its coordination axis allows the H/D exchange on the amine ligand to take place. Next, the deuteration of the hydride sites occurs through the scrambling of terminal and bridging hydrides as recalled above. Interestingly the intermediate containing the coordinated molecular hydrogen is the key step for the thermally activated transformation of **1** into $HOs_3(CO)_{10}(\mu\text{-}\eta^2\text{-}NH=CPh_2)$, as recently reported by Cabeza et al.[33b] On this ground the formation of the latter product is driven by the elimination of the H_2 molecule which results from the formal coupling of H^+ and H^-.

Conclusions

The geometric and energetic features of the DHB in **1** have been characterized by means of several experimental and theoretical techniques. Combined X-ray, NMR, and theoretical analyses indicate that the H···H distance in **1** ranges from about 1.9 Å in the solid state (1.79 Å in the crystal structure and 1.89 Å in the more reliable H-OPT model from theoretical calculations) to 1.93 Å in the gas phase (theoretical calculation with geometrical optimization) and to 2.00 Å in solution (NMR data). This difference can be ascribed to the following factors:

• easy torsional rotation of the imine group around the N−Os1 bond (see Figure 4) in solution;

• deformation vibrations of the three-osmium cluster which are larger in solution;

• contribution of the crystal packing forces, such as

the weak C−H···OC contacts, to the approaching of the two hydrogens involved in the DHB.

• because of the prevailingly electrostatic nature of the DHB, the value of the X-ray distance between the centers of mass of the electron density of the two hydrogen atoms is expected to be smaller than the distance between the two nuclei.

Experimental IR data and theoretical calculations agree in suggesting a DHB interaction energy of about 2.5 kcal/mol, which is in keeping with that obtained from high-level MO calculations on a series of main group DHB complexes.[8] Despite its weakness, the DHB is responsible for driving the thermal transformation of **1** into the $\mu\text{-}\eta^2\text{-}N=CPh_{2-}$containing derivative, likely through an intermediate species containing a molecular hydrogen.

As far as the nature of the studied DHB is concerned, one may conclude the following.

(a) A prevailing electrostatic component is present, similar to that observed in "normal" hydrogen bonds.

(b) The red shift of the $\nu(N-H)$ stretching and the validity of the Jogansen formula[38] also suggest a "normal" behavior of this DHB.

(c) The relatively large polarization component,[9] related to the high polarizability of the M−H bond, seems to be the most typical feature of this "unconventional" dihydrogen bond. This is not surprising because the H of M−H cannot exploit other interaction mechanisms, because no π-systems or lone pairs are available.

Finally from our study it can be concluded that, when stronger "normal" hydrogen bonds are not present, weaker "unconventional" interactions, such as DHB, become important in driving the stereochemistry of the resulting products.